

大面源红外定标器热适配结构优化设计与验证

费志禾¹, 徐 骏¹, 兰少飞¹, 周晓东², 王孝东²

(1. 上海卫星装备研究所, 上海 200240;

2. 上海航天技术研究院, 上海 201109)

摘 要: 针对红外定标器在定标试验过程中因异质材料线膨胀系数不匹配导致结构热失配, 造成低温状态下螺栓松动、降温速率慢、温度均匀性差, 高温状态下玻璃钢隔热垫压溃等问题, 开展大面源、宽温区、多材料体系红外定标器热适配结构优化设计与验证。从法向预紧力调控和面内翘曲变形控制两方面, 筛选关键材料, 调整装配参数, 优化结构参数。采用仿真与试验相结合的手段, 探究高低温状态下异质多层结构螺栓预紧力变化规律, 验证红外定标器结构安全性和稳定性。最后通过升降温试验验证红外定标器关键技术指标。研究表明, 选用聚四氟乙烯作为隔热材料, 配合不锈钢螺栓, 施加初始拧紧力矩介于 10~18 N·m 之间, 调整安装孔径为 25 mm 以上, 可有效控制预紧力变化, 减小面内翘曲变形。全系统仿真结果表明在高低温状态下, 连接安全有效的螺栓比例均达到了 90% 以上。热适配结构设计与优化可显著提高红外定标器降温速率, 改善辐射面低温状态温度均匀性, 结构安全性与稳定性满足设计要求。热适配结构优化设计方法可作为同类产品的参考。

关键词: 红外定标器; 热适配结构; 预紧力; 翘曲变形

中图分类号: TN21 **文献标志码:** A **DOI:** 10.3788/IRLA20220463

0 引 言

卫星红外载荷是卫星实现对地观测的关键设备, 随着定量遥感精度的不断提升, 对卫星红外载荷的辐射定标精度要求也在不断提高^[1-3]。红外定标器作为卫星红外载荷发射前定标的辐射标准, 其精度将直接影响红外载荷的探测精度, 是目前国内外常用黑体辐射源作为卫星载荷的标准红外定标器^[4-6]。红外定标器以普朗克辐射定律为理论基础, 依据自身发射的标准亮度温度信号, 建立输入光通量和探测器输出电信号之间的定量关系^[7]。大口径、大视场、高精度红外光学卫星技术的发展, 对大面源红外定标器定标精度提出了更高的要求。

提高定标精度一方面要求定标器辐射面充分接近理想黑体, 另一方面要求定标器具备足够高的温度精度, 包括高温度均匀性、高控温稳定性、低测温不确定度等, 这就要求定标器整体结构具有稳定、良好的热传递途径, 能实现高均匀度、高精度、高稳定的

温度控制^[8-10]。红外定标器一般通过不同功能层层层压紧, 实现有效传热和精确控温。真空条件下影响层间传热的主要因素是接触热阻。高低温环境中, 异质多层结构与连接螺栓由于热膨胀性能不匹配会发生热失配现象, 导致螺栓预紧力变化。预紧力过大会造成结构变形甚至破坏, 改变定标器传热路径, 温度均匀性下降; 预紧力松弛则会造成功能层之间接触热阻增大, 导致降温速率下降, 试验成本增加。某型号红外定标器研制过程中暴露出低温状态下螺栓松动、降温速率慢、温度均匀性差, 高温状态下玻璃钢隔热垫压溃等问题, 需要对红外定标器开展热适配结构优化设计, 提升性能指标, 保证连接可靠性、安全性。

目前, 国内外学者针对异质多层体系热失配问题^[11]从理论计算、仿真分析^[12]、试验验证^[13]等方面展开了较为深入的研究, 探究螺栓连接预紧力松弛的温度依存行为, 并提出螺栓连接热适配技术。红外定标器具有面积大、温度范围广且同时涉及高低温状态、材料

收稿日期: 2022-09-10; 修订日期: 2022-10-15

基金项目: 国家重点研发计划 (2017YFA0204600)

作者简介: 费志禾, 女, 工程师, 硕士, 主要从事空间材料与制造方面的研究。

体系多等特点,采用热适配技术开展红外定标器力热协同优化设计还未见报道。文中基于工程实际,解决研制过程中暴露的科学问题。从法向预紧力调控和面内翘曲变形控制两方面开展定标器热适配结构设计,筛选关键材料,调整装配参数,优化结构参数。采用仿真与试验相结合的手段,探究高低温状态下异质多层结构螺栓预紧力变化规律,验证红外定标器结构安全性和稳定性。最终通过升降温试验验证红外定标器关键指标。

1 红外定标器结构

大面源红外定标器常采用多层压紧的结构形式,实现辐射、传热和承载功能。整体结构如图 1 所示,包括辐射面、加热层、热平衡层、制冷层、隔热层以及支撑骨架。其中辐射面选用紫铜材料,保证辐射面均温性;加热层为柔性聚酰亚胺加热片;热平衡层由隔热材料和铜板组成,缓解制冷层对辐射板的冷冲击;制冷层为一体化铝质内槽道结构;支撑骨架选用不锈钢材料,是定标器主要支撑和防护部件。定标器使用环境为真空下-100~140 ℃,涉及材料种类多,需进行热适配结构优化设计,保证整体结构稳定性和传热有效性。

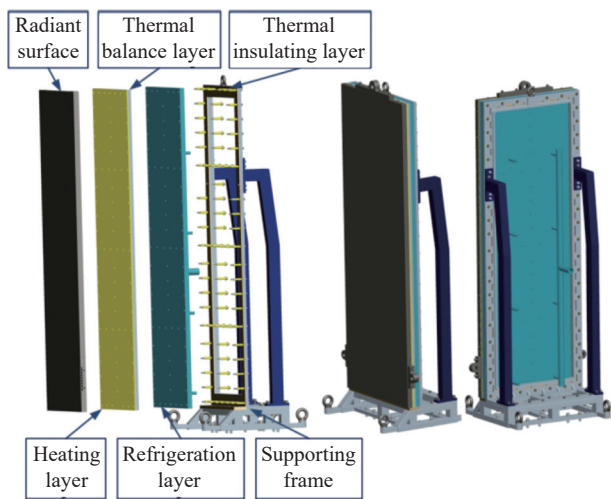


图 1 红外定标器结构

Fig.1 Structure of infrared calibrator

2 法向预紧力调控

在不同温度下,被连接件厚度方向变形与螺栓变形不匹配导致螺栓预紧力发生变化。当温度降低时,

被连接件收缩变形量大于螺栓收缩变形量,预紧力减小;温度升高时,被连接件膨胀变形量大于螺栓膨胀变形量,预紧力增大。图 2 为螺栓连接多层结构示意图。

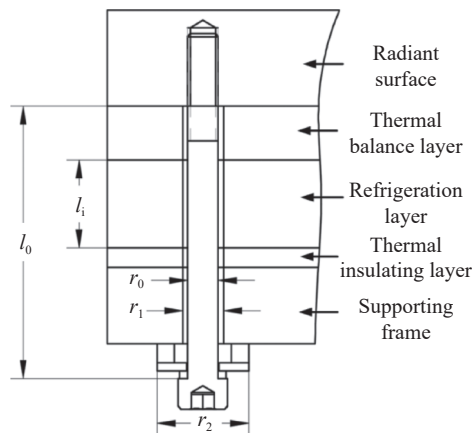


图 2 螺栓与多层结构连接示意图

Fig.2 Schematic diagram of bolted multi-layer structure connection

假设所有材料产生的温度变形均在其弹性范围内,材料热膨胀系数不随温度变化。对定标器在温度 t_0 下施加初始预紧力,考察温度 t 时预紧力变化。预紧力变化过程应满足变形协调条件,即:

$$\delta_t = \delta_F \tag{1}$$

式中: δ_t 为螺栓与被连接件之间的热膨胀相对变形量; δ_F 为预紧力变化产生的螺栓变形量与被连接件变形量之和。

$$\left| \alpha_0 l_0 - \sum_{i=1}^n \alpha_i l_i \right| (t - t_0) = \frac{\Delta F}{C_0} + \frac{\Delta F}{K} \tag{2}$$

式中: α_0 为螺栓材料线膨胀系数; α_i 为多层结构中第 i 层材料线膨胀系数; n 为被连接件层数; 螺栓钉头到辐射板结合面的长度 l_0 应等于所有层板厚度之和,即 $l_0 = \sum_{i=1}^n l_i$; ΔF 为预紧力变化值,工程上常通过力矩法测试拧紧力矩变化评价预紧力变化; C_0 为螺杆轴向刚度,螺栓连接段可简化为圆柱体结构; K 为被连接件轴向刚度,可通过压缩试验测得力-位移曲线获得。

因功能限制,不宜在定标器结构上作改变,亦不适合采用热适配螺栓连接,需从关键材料筛选、装配参数选择两方面调控法向预紧力,提升结构热稳定性。

2.1 关键材料筛选

热适配需要螺栓和被连接材料热膨胀性能相匹配,而被连接材料中隔热材料的选择是热适配设计的

关键。对不同材料组合进行对比分析, -100 °C 下拧紧力矩变化如表 1 所示。可以发现隔热材料选择聚四氟乙烯, 螺栓选用不锈钢时, 拧紧力矩变化较小。这主要是由于不锈钢螺栓相对钛合金螺栓热膨胀系数更高, 同时轴向刚度更大, 而聚四氟乙烯热膨胀系数小于硅橡胶。选择不锈钢与聚四氟乙烯的组合, 可使螺栓与被连接件之间的热膨胀相对变形量较小, 由温度变化导致的预紧力变化更小, 结构相对更稳定。

表 1 -100 °C 下不同材料组合螺栓拧紧力矩变化

Tab.1 Changes of bolt tightening torque with different materials at -100 °C

Heat insulation material	Bolt material	Relative deformation of thermal expansion/mm	Changes of bolt tightening torque/N·m
Silicone rubber	Stainless steel	0.27	13.4
Teflon	Stainless steel	0.14	10.4
Silicone rubber	Titanium alloy	0.35	14.5
Teflon	Titanium alloy	0.22	12.5

2.2 装配参数选择

定标器材结构与材料确定后, 初始拧紧力矩的选择同样会影响结构热稳定性。施加不同初始力矩, 剩余拧紧力矩及螺栓轴向应力如表 2 所示。当初始拧紧力矩为 10 N·m 甚至更小时, -100 °C 剩余拧紧力矩为 0, 螺栓松动。当初始拧紧力矩为 22 N·m 甚至更大时, 高温状态螺栓轴向拉应力大于 6.8 级碳素合金钢螺栓屈服极限的 80%, 螺栓可能变形。因此, 初始拧紧力

表 2 施加不同初始力矩螺栓剩余拧紧力矩及轴向应力

Tab.2 Residual bolt tightening torque and axial stress when applying different original tightening torque

Original tightening torque/N·m	-100 °C		Bolt axial stress/MPa
	Residual tightening torque/N·m	Residual tightening torque/N·m	
10	0	20.4	253.6
12	1.6	22.4	278.5
14	3.6	24.4	303.4
16	5.6	26.4	328.2
18	7.6	28.4	353.1
20	9.6	30.4	378.0
22	11.6	32.4	402.8

矩应介于 12~20 N·m 之间。

2.3 高低温预紧力变化规律

采用单螺栓压紧结构测试高低温预紧力变化, 验证材料选择的正确性, 明确初始拧紧力矩的选择范围, 并探究高低温状态下异质多层结构螺栓预紧力变化规律。单螺栓压紧结构如图 3 所示。试验过程中, 在室温 20 °C 施加初始拧紧力矩, 分别升降温至 140 °C / -100 °C 后, 回复至室温 20 °C, 测试不同温度下的剩余拧紧力矩。



图 3 单螺栓压紧结构试验件

Fig.3 Compressed structure with single bolt

螺栓变形及拧紧力矩变化如图 4 所示。从图中可以发现以下规律:

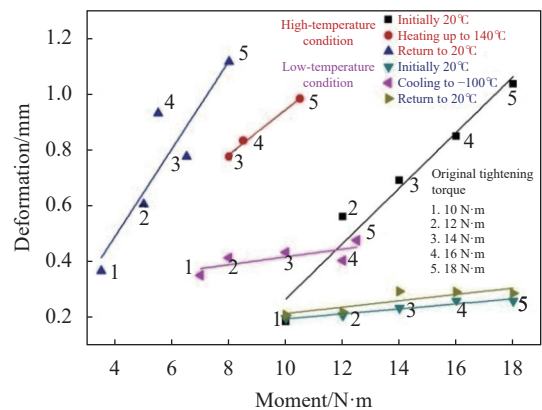


图 4 高低温条件下螺栓变形及拧紧力矩

Fig.4 Bolt deformation and tightening torque at the high and low temperatures

(1) 采取上述材料设计方案, 初始拧紧力矩取 10~18 N·m, 满足结构热适配要求。

(2) 一定范围内, 变形与拧紧力矩呈线性关系, 其斜率可表征多层结构轴向刚度。斜率越大表示该温

度条件下多层结构轴向刚度越小。

(3) 低温工况下, 拧紧力矩变小, 恢复至室温时, 拧紧力矩可恢复。温度变化过程中多层结构轴向刚度几乎不变。表明经过低温工况, 材料属性以及结构特征 (配合间隙等) 未发生变化。

(4) 高温工况下, 拧紧力矩比初始状态更低, 可能是高温状态下材料热膨胀系数非线性变化以及材料的高温蠕变导致的^[14]; 经高温工况, 拧紧力矩减小, 主要是由于聚四氟乙烯板在高温应力作用下发生了一定的塑性变形。

(5) 反复升降温使层板相互挤压, 层与层之间贴合度变优, 多层结构轴向刚度提高。

3 面内翘曲变形控制

由于不同材料热膨胀系数差异, 多层结构在温度变化过程亦会发生面内收缩或膨胀, 导致层板翘曲。不同功能层上的螺栓安装孔在温度载荷作用下的位移不同, 会对螺栓产生剪切作用。功能层材料中聚四氟乙烯与其他材料热膨胀系数差异最大, 温度载荷造成的翘曲变形和对螺栓的剪切力最大。通过调整聚四氟乙烯板安装孔参数, 以适应异质多层结构热胀冷缩。

红外定标器采用 M8 螺栓连接不同功能层, 螺栓外套 14 mm 隔热套, 防止螺栓位置漏热。根据红外定标器设计尺寸与安装状态, 以辐射面变形为基准, 以

距离中心最远的安装孔为对象, 计算从 20 °C 降温至 -100 °C, 不同功能层安装孔在重力与温度载荷作用下, 孔径和孔位变化, 结果如表 3 所示。不考虑层与层之间摩擦力, 聚四氟乙烯板上孔径应大于 37.3 mm, 铝合金制冷板上孔径应大于 15.9 mm, 隔热套不与通孔边缘接触, 此时通孔边缘变形和剪切应力均为零。

表 3 安装孔在温度变化和重力作用下的变形

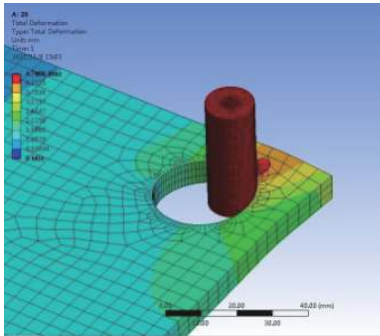
Tab.3 Deformation of mounting holes under temperature changes and gravity

Functional layer and materials	Thickness/mm	Diameter change/mm	Hole location change/mm
Heat insulation layer (Teflon)	8	0.21	13.96
Radiating surface (Copper)	25	0.03	2.32
Refrigeration layer (Aluminum)	23	0.05	3.25

实际情况下, 安装孔孔径过大对安装稳定性以及多层板传热均匀性不利, 应考虑在螺栓剪切力承受范围内, 一定程度扩大安装孔孔径即可。螺栓最大剪切应力发生在聚四氟乙烯与铜板交界处, 由聚四氟乙烯板孔壁承担主要变形。针对聚四氟乙烯板采用不同孔径安装孔, 螺栓受力以及变形情况进行计算, 如表 4 所示。6.8 级螺栓承受静载荷时, 许用切应力为 192 MPa, 将聚四氟乙烯安装孔孔径增大至 25 mm 以上, 可满足螺栓剪切安全要求。

表 4 安装孔孔径对螺栓剪切应力与变形的影响

Tab.4 Effects of mounting hole diameter on shear stress and deformation of bolt

Displacement fringe at -100 °C	Mounting hole diameter/mm	Shear stress/MPa	Deformation/mm
	17	313.34	0.015
	22	215.66	0.008 6
	25	160.4	0.006 5
	28	110.25	0.004 3
	30	83.61	0.003 2

4 红外定标器全系统仿真分析

通过有限元仿真, 分析高低温条件下红外定标器

的整体变形与应力分布。以 20 °C 为参考温度, 对定标器施加重力载荷和温度载荷。红外定标器整体变

形如图 5 所示。从变形分布图可以看出,高温状态下,定标器轻微往前凸,低温状态下,定标器轻微往后凹,

整体变形最大为 7.1 mm,造成的弯矩小于 28.4 N·m,结构热变形不足以导致定标器倾覆。

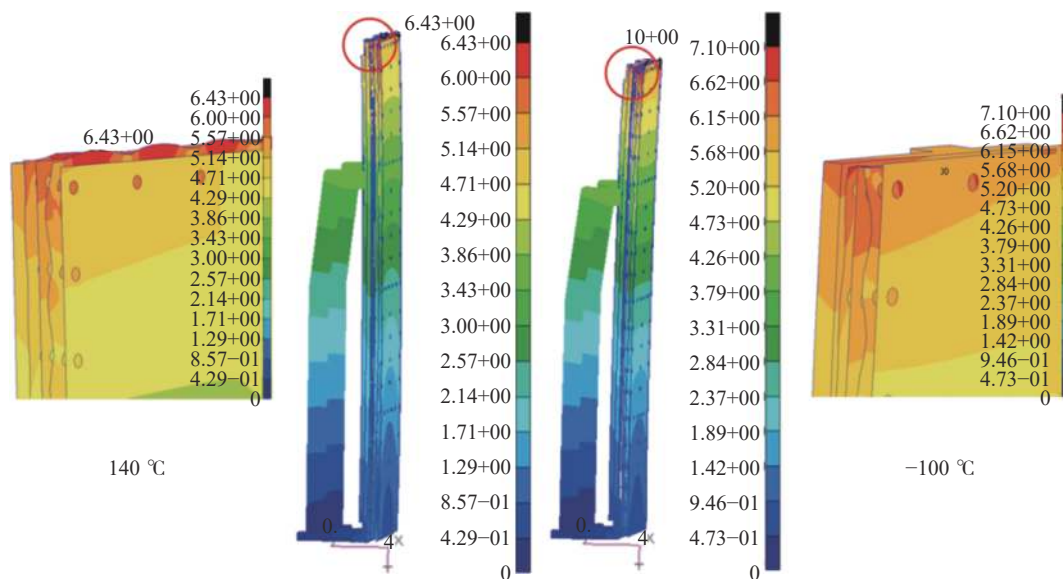


图 5 高低温条件下红外定标器位移云图

Fig.5 Displacement fringe of infrared calibrator at high and low temperatures

由于不同材料热膨胀系数差异,功能层材料尤其是聚四氟乙烯板会发生褶皱,面内变形与厚度方向变形的耦合造成不同位置的螺栓预紧力变化不一致。分析定标器螺栓轴向应力可以发现,上下边缘的螺栓应力随温度变化明显大于其他位置。层板的褶皱变形使得高低温情况下均有部分螺栓松弛或涨紧,不同状态螺栓占总螺栓数比例如表 5 所示。高低温状态下,连接安全有效的螺栓比例均达到了 90% 以上。可根据不同位置螺栓拧紧力矩变化,制定差异化装配参数,即适当提高低温松动螺栓的初始拧紧力矩,适当降低高温涨紧螺栓的初始拧紧力矩,进一步提高安全螺栓的比例。

5 红外定标器升降温试验

红外定标器升降温试验是确定定标器研制过程中的技术方案合理性和指标符合度的主要方法。基于前期工艺参数摸索,完成了红外定标器系统集成,并利用真空罐开展升降温试验。针对降温速率、温度均匀性、结构稳定性等开展全方位工艺验证。试验过程如图 6 所示。

表 5 不同状态螺栓比例

Tab.5 Proportion of bolts in different states

Temperature/°C	Residual tightening torque				Safe and effective connection
	0 N·m	0-2 N·m	>28 N·m	>30 N·m	
	Loose	Relaxation	Inflation	Deformation	
140	2.56%	0	2.56%	0	94.9%
-100	3.85%	2.56%	0	0	93.6%

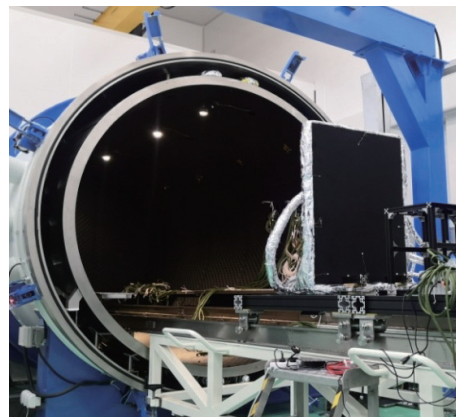


图 6 红外定标器升降温试验

Fig.6 Heating and cooling test for infrared calibrator

在热边界条件一致的情况下,分别对结构优化前后红外定标器降温速率进行测试。为了排除制冷板

制冷功率对降温速率的影响,截取结构优化前后两次高低温试验过程中部分降温曲线(从 273 K 降到 193 K)分析降温速率,选取的两次降温过程中制冷板功率保持一致。降温曲线如图 7 所示,可以发现经过热适配结构优化设计,降温时间从 30 h 缩短为 4 h,传热效率得到了显著提高。红外定标器温度均匀性通过在辐射面上均匀分布的 Pt100 测温传感器进行实时温度测量得到,其测温精度优于 0.1 K,测温分辨率优于 0.01 K。对结构优化前后低温状态温度均匀性进行了测试,辐射面在 193 K 温度偏差从 $-0.8\text{ K}/+0.9\text{ K}$ 提升为 $-0.3\text{ K}/+0.4\text{ K}$,温度均匀性明显改善。试验完成后对定标器进行拆解,定标器结构、螺栓及垫片等无明显变形和破坏。升降温试验表明定标器结构安全稳定,降温速率、温度均匀性等满足设计指标。

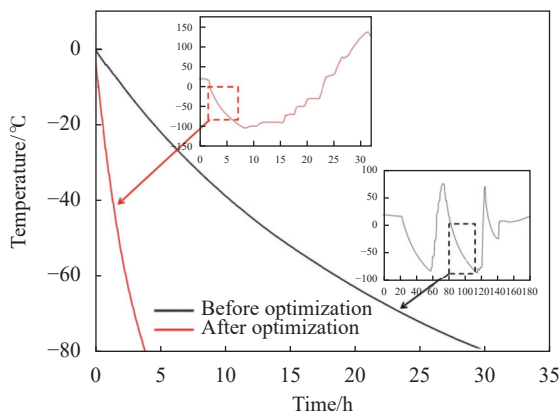


图 7 优化前后降温速率对比

Fig.7 Comparison of cooling rate before and after optimization

6 结 论

针对红外定标器研制过程中暴露的问题,开展了大面源、宽温区、多材料体系红外定标器热适配结构优化设计与验证。通过关键材料筛选和装配参数选择调控法向预紧力,选择聚四氟乙烯作为隔热材料,选用不锈钢螺栓,确定初始拧紧力矩应介于 10~18 N·m 之间。通过优化结构参数,调整安装孔孔径为 25 mm 以上,减小定标器面内翘曲变形。探究了高低温预紧力变化规律,经过低温工况预紧力可恢复,经过高温工况预紧力减小。全系统仿真结果表明,在高低温状态下连接安全有效的螺栓比例均达到了 90% 以上。可根据不同位置螺栓拧紧力矩变化,制定差异化装配参数。升降温试验结果表明热适配结构

设计与优化可显著提高红外定标器降温速率,改善辐射面低温状态温度均匀性,结构安全性与稳定性满足设计要求。大面源红外定标器热适配结构优化设计方法可作为同类产品的参考。

参考文献:

- [1] Sheng Y C, Dun X, Jin W Q, et al. Review of on-orbit radiometric calibration technology used in infrared remote sensors [J]. *Infrared and Laser Engineering*, 2019, 48(9): 0904001. (in Chinese)
- [2] Wang C L, Wang C Y, Gu J, et al. An improved non-uniformity correction algorithm based on calibration [J]. *Chinese Optics*, 2022, 15(3): 498-507. (in Chinese)
- [3] Li J, Zhao J K, Chang M, et al. Radiometric calibration of photographic camera with a composite plane array CCD in laboratory [J]. *Optics and Precision Engineering*, 2017, 25(1): 73-83. (in Chinese)
- [4] Ogarev S A, Morozova S P, Katysheva A A, et al. Blackbody radiation sources for the IR spectral range [J]. *AIP Conference Proceedings*, 2013, 1552(1): 654-659.
- [5] Ljungblad S, Holmsten M, Josefson L E, et al. Comparison of blackbody sources for low-temperature IR calibration [J]. *International Journal of Thermophysics*, 2015, 36(12): 3310-3319.
- [6] Liu J C, Li H W, Wang J L, et al. Combined radiometric calibration of ground-based large-aperture infrared photoelectric systems [J]. *Optics and Precision Engineering*, 2017, 25(10): 2541-2550. (in Chinese)
- [7] Zhao X Y. The study of radiometric calibration for staring camera with large diameter[D]. Harbin: Harbin Institute of Technology, 2010. (in Chinese)
- [8] Liang C, Ma T X. Design of infrared imaging nonuniformity correction system based on black body calibration [J]. *Chinese Optics*, 2016, 9(3): 385-393. (in Chinese)
- [9] Yang C P, Xu K, Xue L, et al. Temperature control technology for extra large surface blackbody based on two-phase fluid [J]. *Infrared and Laser Engineering*, 2022, 51(12): 20220195. (in Chinese)
- [10] Kim H I, Chae B G, Choi P G, et al. Thermal design of blackbody for on-board calibration of spaceborne infrared imaging sensor [J]. *Aerospace*, 2022, 9(5): 268.
- [11] Luo S K, Cheng G M. Thermal adapter of HgCdTe large plane arrays detector based on carbon fiber with high heat conductivity used in infrared space camera [J]. *Infrared and Laser*

- Engineering*, 2016, 45(7): 0704001. (in Chinese)
- [12] Lin R X, Dang W T, Li Y F. Optimization and analysis of pre-tightening force on connection bolts [J]. *Journal of Chengdu University (Natural Science)*, 2018, 37(4): 416-418. (in Chinese)
- [13] Pei R G, Xiao Y, Chen H L, et al. Temperature-time dependent behavior for preload relaxation in bolted composite joints [J]. *Acta Materiae Compositae*, 2016, 33(4): 768-778. (in Chinese)
- [14] Li N, Zhou J H, Zhang F P, et al. Study of preload change rules under high temperature for rotor system of missile turbofan engine [C]//6th China Joint Conference on Aerospace Propulsion, 2021: 740-748.

Optimal design and verification of thermal adaptive structure for infrared calibrator with large surface

Fei Zhihe¹, Xu Jun¹, Lan Shaofei¹, Zhou Xiaodong², Wang Xiaodong²

(1. Shanghai Institute of Satellite Equipment, Shanghai 200240, China;

2. Shanghai Academy of Spaceflight Technology, Shanghai 201109, China)

Abstract:

Objective Infrared calibrators directly determine the detection accuracy of infrared devices as the reference standard for radiation measurement of infrared devices before the satellite launching. More precise infrared calibrators with large surface are required with the development of infrared optical satellites characterized by large aperture, large field of view and high precision, which means the structure of infrared calibrators must keep stable in high and low temperatures to guarantee the high temperature uniformity of the radiant surface, high precision of temperature control and high stability of the system. In the calibration test, the structure thermal mismatch easily occurs because the multilayered structure of infrared calibrators connected with bolts usually includes a variety of different materials and the deformations become unmatched during heating and cooling process for different thermal expansivity, which can reduce the calibration accuracy and increase security risks and test cost. As a result, optimal design and verification of thermal adaptive structure for the infrared calibrator with large surface, wide temperature range and multiple materials were carried out, to solve the problems caused by structure thermal mismatch, including the loose bolts, low cooling rate and bad thermal uniformity at the low temperatures, as well as the compression failure of heat insulating mattress made of glass reinforced plastic at the high temperatures.

Methods From the two aspects of normal preload regulation and in-plane warping deformation control, the key materials were selected, the assembly parameters were adjusted and the structure parameters were optimized. Simulation analysis and tests were combined to explore the change rules of bolts preload on multilayered structure made of different materials when the temperature changed, at the same time verify the safety and stability of the structure. Finally, the key technical indexes of infrared calibrator were verified by means of heating and cooling tests.

Results and Discussions The calculations based on the linear elastic theory indicated that the change of preload was controlled effectively by means of choosing Teflon as heat insulation material and stainless steel as bolt material (Tab.1), which provided a smaller relative deformation between bolts and connected members caused by the temperature change. The original preload was applied between 12 N·m to 20 N·m to avoid bolts looseness at -100 °C and deformation failure at 140 °C (Tab.2). Furthermore, the diameters of mounting holes were enlarged to be greater than 25 mm to reduce the in-plane warping deformation resulting from bolts shearing (Tab.3). The tightening torque test based on multilayered structure composed of different materials discovered the rules that the

tightening torque got linear relation with the deformation in the certain range. The elastic deformation occurred at the low temperatures and on the other hand the plastic deformation was more likely to occur at the high temperatures. The axial stiffness of multilayered structure could be improved by repeating heating and cooling process (Fig.4). The simulation result of the whole system suggested that the proportion of bolts with safe and effective connections had reached more than 90% under the high and low temperatures (Tab.3). The stress of bolts at the upper and lower edges of the calibrator changed more significantly than that at other positions and therefore different assembly parameters could be set according to the bolt positions. The heating and cooling test of infrared calibrator showed that the structure was safe and stable with the temperature change, the cooling time was shortened from 30 h to 4 h (Fig.7), and the temperature deviation of the radiant surface at 193 K was improved from $-0.8\text{ K}/+0.9\text{ K}$ to $-0.3\text{ K}/+0.4\text{ K}$.

Conclusions The optimal design of thermal adaptive structure can significantly increase the cooling rate of infrared calibrator and improve the thermal uniformity of radiant surface at the low temperatures. The difficulties of loose bolts at the low temperatures and compression failure of heat insulating mattress at the high temperatures were overcome at the same time. This study solved the practical problems in the calibration test and the structural safety and stability after optimal design can meet the design requirements. The optimal design methods of thermal adaptive structure can be referred for the same type of products.

Key words: infrared calibrator; thermal adaptive structure; preload; warping deformation

Funding projects: National Key Research and Development Program of China (2017YFA0204600)